CILASCI

5

5º CONGRESSO IBERO-LATINO-AMERICANO EM SEGURANÇA CONTRA INCÊNDIOS

5th IBERIAN-LATIN-AMERICAN CONGRESS ON FIRE SAFETY

15-17 /07/ 2019 - Porto, Portugal

Atas dos Artigos
Proceedings (full papers)

ipb INSTITUTO POLITÉCNICO DE BRAGANÇA
U.PORTO FEUP FACULDADE DE ENGENHARIA UNIVERSIDADE DO PORTO
isep Instituto Superior de Engenharia do Porto
albrasci

CILASCI
5

5º CONGRESSO IBERO-LATINO-AMERICANO EM SEGURANÇA CONTRA INCÊNDIOS

5th IBERIAN-LATIN-AMERICAN CONGRESS ON FIRE SAFETY

15-17 /07/ 2019 - Porto, Portugal

Atas dos Artigos
Full Papers Proceedings

5th IBERIAN-LATIN-AMERICAN CONGRESS ON FIRE SAFETY – CILASCI 5
Porto, Portugal, 15 - 17 July 2019

TITLE:
Atas dos Artigos
5º Congresso IBERO-LATINO-AMERICANO EM SEGURANÇA CONTRA INCÊNDIOS

Full Papers Proceedings
5th IBERIAN-LATIN-AMERICAN CONGRESS ON FIRE SAFETY

PUBLISHER:
ALBRASCI - Associação Luso-Brasileira para a Segurança Contra Incêndio
ALBRASCI - Luso Brazilian Association for Fire Safety

EDITORS:
Paulo Piloto (IPB - DMA), Débora Ferreira (IPB - DMA), Elza Fonseca (ISEP - DEM), João Santos Baptista (FEUP-DEM), José Miguel Castro (FEUP – DEC), Luís Mesquita (IPB - DMA), Mário Vaz (FEUP-DEMec), Miguel Chichorro (FEUP – DEC), Rui Miranda Guedes (FEUP-DEMec) et al.

BOOK COVER DESIGN:
Soraia Maduro – Instituto Politécnico de Bragança

INTERNET WEB PAGE:
Pedro Oliveira – Instituto Politécnico de Bragança

EDITION:
1ª, Julho de 2019

ISBN:
978-989-97210-3-6

IMPRINT:
Tipografia Artegráfica Brigantina

PREFACE

The Iberian-Latin American Congress on Fire Safety (CILASCI) is held once every two years, with the aim of disseminating scientific and technical knowledge in the field of fire safety, integrating different players involved in this area of knowledge. The first edition of the Iberian-Latin American Congress on Fire Safety (CILASCI 1), was held in Natal (Brazil) between 10-12 March 2011. The second congress (CILASCI 2) was held in Coimbra (Portugal), between May 29 and June 1, 2013. The 3rd and 4th editions took place on the South American continent. The third congress (CILASCI 3) was held in Porto Alegre (Brazil) from November 3 to 6, 2015, while the fourth congress (CILASCI 4) was held in Recife (Brazil) from 9 to 11 October 2017. The CILASCI 5 will take place in the city of Porto (Portugal) from 15 to 17 July 2019, and presents 5 invited lectures and 78 manuscripts (full papers) from researchers around the world (Algeria, Australia, Belgium, Brazil, China, Czech Republic, France, Hong Kong, Italy, Mozambique, Portugal, Spain, United Kingdom and United States).

the 5th Iberian-Latin-American congress on fire safety reflects the new developments achieved on active and passive fire protection, on evacuation and human behaviour under fire, on computational modelling of structures and materials under fire, on explosion and risk management, on architectural issues for fire safety in buildings, on fire dynamics, on the experimental analysis of materials and structures under fire, on fires in special buildings and spaces, on fire-fighting operations and equipments, and on the behaviour of structures and materials under fire.

The Fire Safety is reaching new developments as a result of new research, development and innovation around the world, based on the excellence level of the research, the support of new skilled professionals and due to the existence of advanced training programmes in fire science technology. This development will increase the safety level of people, buildings, and products, but also is going to produce an impact in the economy of each country, with a positive impact on society.

The organizing committee believe that this congress will address to our delegates a wide forum of discussion about the recent developments in Fire Safety, promoting the exchange of ideas and international cooperation.

The organizing Committee would like to thanks to all authors and delegates.

On the behalf of the Organizing Committe
Paulo A. G. Piloto

ORGANIZING COMMITTEE

SCIENTIFIC COMMITTEE

INDEX

INVITED LECTURES

INVITED LECTURE P1:
EMERGENCY EXITS IN HIGH RISE BUILDINGS
Rosaria Ono, University of São Paulo

INVITED LECTURE P2:
THE NEW GENERATION OF PARTS 1-2 (STRUCTURAL FIRE DESIGN) OF EUROCODES 1, 3 AND 4
Paulo Vila Real, University of Aveiro

INVITED LECTURE P3:
CHARACTERIZATION OF THE FIRE REACTION OF MATERIALS
Daniel Alvear, University of Cantabria, GIDAI

INVITED LECTURE P4:
ADVANCES IN FIRE PROTECTION TECHNOLOGIES
Sergey Dorofeev, FM GLOBAL

INVITED LECTURE P5:
SMOKE CONTROL IN COMPARTMENTS: SIMULATION AND EXPERIMENTS
João Viegas, National Laboratory for Civil Engineering

5th IBERIAN-LATIN-AMERICAN CONGRESS ON FIRE SAFETY – CILASCI 5
Porto, Portugal, 15 - 17 July 2019

EFFECT OF THE LOAD LEVEL IN THE FIRE RESISTANCE OF COMPOSITE SLAB WITH STEEL DECKING

Carlos Balsa *
Professor
IPB
Bragança

Lucas Santos
Student
UTFPR
Brazil

Paulo A. G. Piloto
Professor
IPB
Bragança

Érica Kimura
Professor
UTFPR
Brazil

Keywords: Composite slabs; Fire resistance; Experimental tests, Numerical validation; Standard Fire.

1. INTRODUCTION

The composite slab with steel decking is widely used in every type of buildings. A composite slab consists of cold-formed profiled steel deck which acts as a permanent formwork to the concrete topping. Normally, this composite solution requires the addition of other components such as steel rebars (placed within the ribs) for positive bending and steel mesh for negative bending, preventing cracks in concrete, see Figure 1. Due to the external reinforcement provided by the steel deck, composite slabs generally require less additional reinforcement and less concrete as well, resulting in slender slabs. In addition, the reduction of the construction time, elimination or reduction of struts and the simplicity of installation, are other advantages of composite slabs in comparison to conventional flat concrete slabs. The composite action between the concrete and the steel deck is generally achieved by indentations or embossments in the steel deck.

Since 1980, a significant increase in the use of composite slabs has taken place. The overall depth usually varies between 100 and 170 mm. Several types of steel deck are marketed in

*Autor correspondente – Dep. de Matemática, Insituto Politécnico de Bragança. Campus Santa Apolónia, 5300-253 Bragança.
Telef.: +351 273 303000, Fax: +351 273 313051, E-mail: balsa@ipb.pt

Europe, with a thickness varying between 0.7 and 1.2 mm, usually made from galvanized steel to increase durability [1].

Composite slabs have to meet fire-safety requirements in accordance to standards and regulations. Generally, standard fire tests using the standard fire curve ISO 834 [2] are utilized for determining the fire rating of this structural element, accounting for Load Bearing (R), Integrity (E) and Insulation (I).

Throughout the years of 1989 and 1993 more than 30 full scale fire resistance tests were carried out on a wide range of structural assemblies on the United Kingdom, demanded by the Steel Construction Institute, and those were summarized in multiple publications [2]. One of those was made by G. Thomson and co-authors [3] concerning standard fire tests on composite steel and concrete slabs, using two types of slab, and two kinds of concrete (normal weight – NWC and light weight – LWC), supported by thermal isolated steel beams capable to resist heat effect for 90 minutes. The test was carried through 120 minutes, the furnace temperature was controlled to follow ISO 834 curve and having the temperatures on slabs and beams profile section measured.

In 2011, Guo & Bailey [4] investigated the thermal and mechanical response of composite slabs using trapezoidal steel decks, during heating and cooling stages, intending to provide data to future researches on thermal resistance and numerical modelling. In their work 7 different situations were analysed, using the same structure but varying fire conditions, loading rates and cooling conditions. Different fire scenarios were used, to differ from the standard fire [2] and the results showed that the velocity of heating and cooling in different loading conditions matters, affecting not only the maximum temperatures in the deep of the slab from the exposed face, but also in the deflections during the tests.

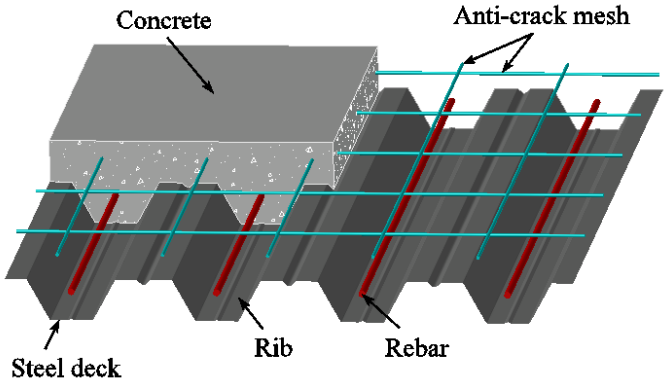

Figure 1: Typical layout of a composite slab with trapezoidal steel deck.

The integrity (E) is the capacity to withstand fire in one side and the assessment should be made on the basis of measuring cracks or openings in excess of given dimensions, or the ignition of a cotton pad, or sustained flaming on the unexposed side or while the load bearing (R) resistance withstands [5]. For cast in situ composite slabs, the integrity criterion is normally satisfied provided that the joints are adequately sealed.

The insulation (I) is the ability to withstand fire in one side and the assessment shall be made on the basis of the average temperature rise on the unexposed face limited to 140 °C above the initial average temperature, or; made on the basis of the maximum temperature rise at any point limited to 180 °C above the initial average temperature.

The load bearing resistance for flexural loaded elements (R) is the ability to support the loading during the test and the assessment shall be made on the basis of limiting vertical displacement D ($D=L^2/400d$ [mm]), or limiting rate of vertical displacement ($dD/dt=L^2/9000d$ [mm/min]), being L the clear span of the testing specimen in millimetres and d is the distance from the extreme fibre of the cold design compression zone to the extreme fibre of the cold design tensile zone of the structural section, in millimetres.

Generally, experimental tests are expensive and time-consuming. As an alternative solution, the fire resistance can be evaluated by means of numerical simulations or using simple calculation methods. The fire resistance of the composite slabs is defined with respect to standard fire exposure from below. The scope of this investigation concerns the fire rating for the R and I criteria. Numerical simulations with finite elements were developed, using ANSYS, to find out the thermal and mechanical effects of standard fire exposure. The results of the numerical simulation are compared with experimental results from Hamerlink [1] and with the simplified method proposed by Eurocode 4-part 1.2 [6].

2. EUROCODE 4: FIRE RESISTANCE OF COMPOSITE SLABS

In this section we present the simplified methods included in standards and regulations used for determining the fire rating of structural element, accounting for Insulation (I) (see [6]) and Load Bearing (R) (see [7] and [5]).

2.1 Fire resistance for insulation (I)

A simplified method is presented in the Annex D of EN 1994-1-2 [6] for the estimation of the fire resistance of unprotected composite slabs subjected to fire exposure from below, using the standard fire curve ISO 834. The analytical expressions present in the current version of this standard are based on the research conducted by Both [8] in 1998. During the last years, no revisions were made to these methods [9]. The fire resistance (I) with respect to thermal insulation criterion shall be determined according to Eq. 1.

$$t_i = a_0 + a_1 \cdot h_1 + a_2 \cdot \phi + a_3 \cdot \frac{A}{L_r} + a_4 \cdot \frac{1}{l_3} + a_5 \cdot \frac{A}{L_r} \cdot \frac{1}{l_3} \quad (1)$$

The rib geometry factor (A/Lr) of the composite slab shall be calculated as follows:

$$A/L_r = h_2 \cdot \left((l_1 + l_2)/2\right) \Big/ \left(l_2 + 2\sqrt{h_2{}^2 + \left((l_1 - l_2)/2\right)^2} \right) \quad (2)$$

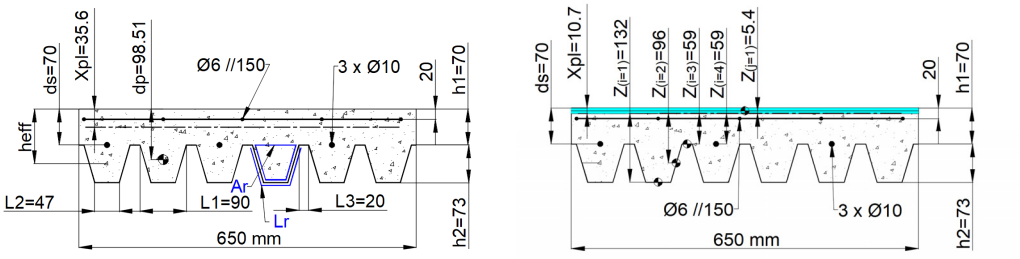

a) Room temperature. b) After 90 minutes of fire.

Figure 2: Model for the composite slab with steel deck.

In addition to the geometric parameters of the composite slab, illustrated in Figure 2, the fire resistance also depends on partial factors (a_i). Table 1 presents these factors for slabs with normal weight concrete (NWC).

Table 1: Coefficients for estimating the fire resistance for NWC (EN 1994-1-2 [6])

a_0 (min)	a_1 (min/mm)	a_2 (min)	a_3 (min/mm)	a_4 (mm min)	a_5 (min)
-28.8	1.55	-12.6	0.33	-735	48.0

The view factor (ϕ) specified in the Eq. (1), quantifies the geometric relation between the surface emitting radiation and the surface receiving, that depends on the surfaces areas and orientations, as well as the distance between them [9]. The view factor at the lower flange of the composite slab is given as $\phi_{lower} = 1$. The view factor of the web ϕ_{web} and of the upper flange ϕ_{upper} of the steel deck are smaller than one, due to the obstruction caused by the ribs of the steel deck. These values can be calculated by Hottel´s crossed-string method, using Eq. (3) and Eq. (4).

$$\phi_{upper} = \frac{\sqrt{h_2^2 + \left(l_3 + \frac{l_1 - l_2}{2}\right)^2} - \sqrt{h_2^2 + \left(\frac{l_1 - l_2}{2}\right)^2}}{l_3} \quad (3)$$

$$\phi_{web} = \frac{\sqrt{h_2^2 + \left(\frac{l_1 - l_2}{2}\right)^2} + (l_3 + l_1 - l_2) - \sqrt{h_2^2 + \left(l_3 + \frac{l_1 - l_2}{2}\right)^2}}{2\sqrt{h_2^2 + \left(\frac{l_1 - l_2}{2}\right)^2}} \quad (4)$$

2.2 Fire resistance for load (R)

Aiming the definition of simple calculation rules of mechanical behaviour and capacity of composite elements made of steel and concrete, the Eurocode 1994-1-2 [6] provides general

rules on the determination of composite steel-concrete slabs load capacity. Based on a global plastic analysis, the design for bending resistance may be determined using Eq. 5.

$$M_{fi,t,Rd} = \sum_{i=1}^{n=4} A_i \; z_i \; k_{y,\theta,i} \left(f_{y,i} / \gamma_{M,fi} \right) + \alpha_{slab} \sum_{j=1}^{m=1} A_j \; z_j \; k_{c,\theta,j} \left(f_{c,j} / \gamma_{M,fi,c} \right) \qquad (5)$$

The coordinates z_i and z_j are the distances of the components for steel and concrete materials, between the geometric centre and the neutral axis of the slab, under fire conditions, see Figure 2. Coefficients $k_{y,\theta,i}$ and $k_{c,\theta,i}$ concern the reduction coefficients for the yielding stress of steel and compressive strength of concrete, affected by the temperature of each component, being defined by standards for steel [10] and concrete [11], using interpolation. $k_{y,\theta,i}$ has different values, according to the type of steel (cold formed carbon steel for the design of class 4 sections at elevated temperatures [6] and cold formed carbon steel for rebars [11]). There is no reduction for concrete.

The neutral axis under fire conditions, can be defined by the equilibrium of Eq. 6, [6]. This axis modifies its position, moving from the hot region to the cold region, see Figure 2 por the position after 90 minutes of fire exposure.

$$\sum_{i=1}^{n=4} A_i \; k_{y,\theta,i} \left(f_{y,i} / \gamma_{M,fi} \right) + \alpha_{slab} \sum_{j=1}^{m=1} A_j \; k_{c,\theta,j} \left(f_{c,j} / \gamma_{M,fi,c} \right) = 0 \qquad (6)$$

After completed the calculation of maximum value, the verification shall be made comparing the maximum bending resistance moment with the effect of the applied bending momentum. In this study, for the case of a simply supported slab with a distributed load (q), the effect of the applied bending moment should be calculated with Eq. 7.

$$M^{+}_{fi,d,t} = q \; L^2 / 8 \qquad (7)$$

3. NUMERICAL SIMULATIONS

In this section, the methodology used to model and solve the thermal and mechanical effects on the composite slab is presented. Therefore, a brief description of the finite elements, thermal and mechanical properties of materials, boundary conditions and convergence criterion is given for both, thermal and mechanical model.

3.1 Thermal model

The composite slab is meshed in order to solve a nonlinear transient thermal analysis, using 3D finite elements from ANSYS. The finite element method (FEM) requires the solution of Eq. 8 in

the domain and the definition of the boundary conditions according to Eq. 9 in the exposed and unexposed side of the slab.

$$\nabla\left(\lambda_{(T)}.\nabla T\right) = \rho_{(T)}.Cp_{(T)}.\partial T/\partial t \tag{8}$$

$$\lambda_{(T)}.\nabla T.\vec{n} = \alpha_c\left(T_g - T\right) + \phi.\varepsilon_m.\varepsilon_f.\sigma.\left(T_g^4 - T^4\right) \tag{9}$$

In the equations above: T represents the temperature of each material; $\rho(T)$ is the specific mass; $Cp(T)$ is the specific heat; $\lambda(T)$ is the thermal conductivity; α_c is the convection coefficient. T_g represents the gas temperature of the fire compartment, using the standard fire ISO 834 applied on the bottom part of the slab; ϕ is the view factor (see previous section); ε_m is the emissivity of each material; ε_f represents the emissivity of the fire and σ represents the Stefan-Boltzmann constant.

The finite element method is applied to solve numerically the heat transfer equation. For an arbitrary composite slab with trapezoidal steel deck, the respective 3D mesh is presented in Figure 3.

The three-dimensional model of the composite slab considers perfect contact between materials, namely the concrete topping, the steel deck, the steel rebars and the steel mesh. The model identified by NUM 0 considers the perfect contact between the steel deck and the concrete. The model identified by NUM 1 considers 1 mm of air gap size, with perfect contact between the air and both surfaces of concrete and steel. A second alternative thermal model, considers the air gap effect with a constant thickness (1 mm), being included between the steel deck and the concrete topping in order to simulate debonding effects.

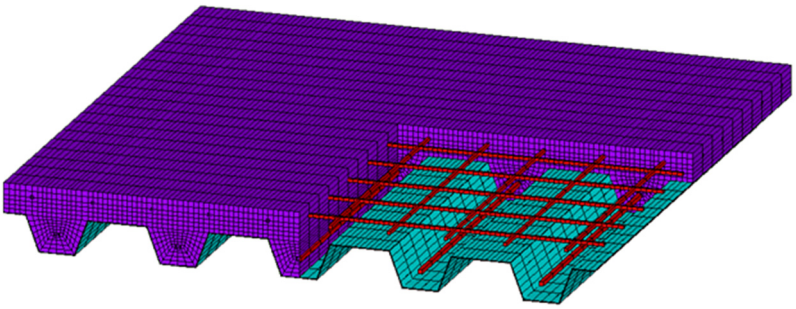

Figure 3: Finite element mesh of a composite slab with trapezoidal steel deck.

For each material, a specific 3D finite element is used. Three different finite elements are used: SHELL131, SOLID70 and LINK33. The SHELL131 element has four nodes with up to 32 degrees of freedom (temperature) in each node, depending on the number of layers (one layer, linear variation, 3 nodal temperatures). Compatibility between nodal shell temperature and nodal solid temperature is guaranteed. This element presents linear interpolating functions in the plane of the element, using full Gauss integration method (2x2) and linear interpolating functions through the layer thickness (three Gauss points). The shell element is used to model the steel deck of the composite slab. The SOLID70 element presents eight nodes with a single degree of freedom

(temperature) at each node. Linear interpolating functions are used for this element and the full Gauss integration method is also applied (2x2x2). This finite element is used to model the concrete topping and, in the second case, the air gap volume. The LINK33 element has two nodes with a single degree of freedom (temperature) per node. This uniaxial element presents linear interpolating functions as well as exact integration. The LINK33 element is used to model the anti-crack mesh and the rebars.

The thermal properties of the materials are temperature dependent and vary according to the standards used for composite slabs, steel structures and concrete structures [5, 7, 8]. The thermal properties of steel and concrete are presented in Figures 4 and 5, respectively. The conductivity of steel decreases with temperature and the specific heat has a strong variation due to the allotropic phase transformation. Both density and conductivity of concrete decrease as the temperature increase. Regarding the conductivity, the upper limit was selected for the numerical simulations. The specific heat of concrete presents a peak value related to 3% of moisture content of concrete weight.

The thermal properties of air are depicted in Figure 6. These properties are also temperature dependent and were used in the air gap to simulate the effects of debonding between the steel deck and the bottom surface of the concrete. This model only considers the heat flow by conduction in the air gap, due to the very small air gap thickness.

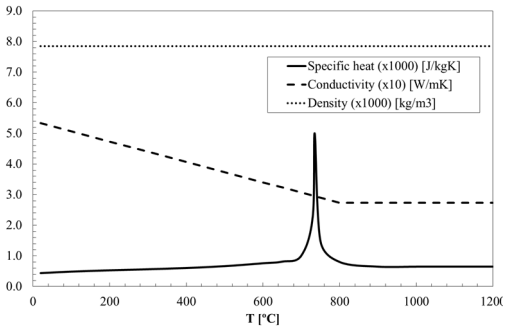

Figure 4: Thermal properties of carbon steel.

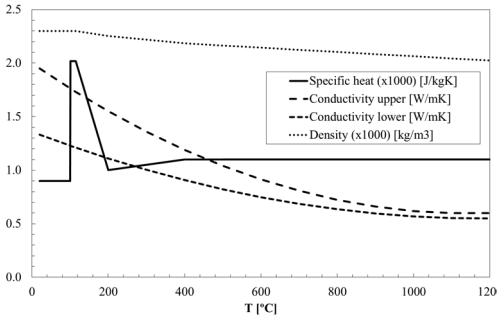

Figure 5: Thermal properties of concrete.

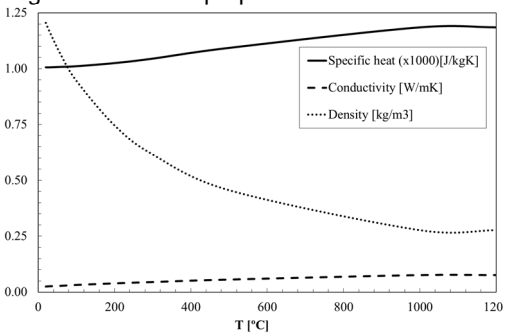

Figure 6: Thermal properties of air.

The exposed side of the slab is submitted to a heat flux by convection and radiation (see Eq. 9) using different values for view factors and a bulk temperature following the standard fire. The unexposed side is subjected to a convective heat flux (including the radiation heat flux), using a constant bulk temperature of 20 ºC, see Figure 7.

All the nodes of the numerical model are set with an initial condition for temperature of 20 °C. The lower part of the steel deck is subjected to standard fire conditions using a convection coefficient of 25 W/m²K and an emissivity of fire equal to 1. A convective coefficient of 9 W/m²K is applied on the upper part of the composite slab in order to include the radiation effect [12]. The main parameters of the applied boundary conditions are illustrated in Figure 7.

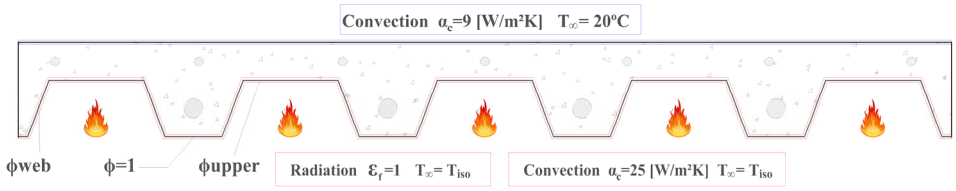

Figure 7. Representation of the applied boundary conditions.

The heat flow criterion was applied for the convergence criterion, using a tolerance value of 0.001 and a minimum reference value of 10^{-6}.

3.2 Mechanical model

The mechanical simulation for the fire behaviour of the composite slabs is also presented. The model is validated using the experimental results from Hamerlinck [1]. The displacement and the rate of displacement are compared with the experimental results and compared with the criterion for fire rating given by EN 1363-1 [7].

The integral value for the surface force over any surface of an arbitrary volume element within the material must sum to zero in order to keep the static equilibrium, in each time step. Here we assume the existence of an external load {F} (live and dead load) on material within the volume submitted to the stress field [σ]. The surface integral can be converted to a volume integral by the Gauss' divergence theorem. The final version of the equilibrium equation may be expressed in every Cartesian coordinate, according to Eq. 10.

$$\nabla[\sigma]+\{F\}=\{0\} \tag{10}$$

The external load {F} is considered to be constant under fire conditions. The load bearing capacity was determined for room temperature, using Eq. 11 for sagging moment resistance and assuming the neutral axis to be located above the steel deck. *Mp,Rd* represents the plastic bending resistance, *Np,pl* the plastic tensile force for the effective section of the plate, *Ns,pl* the plastic

tensile force for rebars, *dp* represents the centroidal position for the plate measured from the top of the cross-section, *xpl* represents the position for the plastic neutral axis measured from the top and *ds* represents the position of the rebars measured from the top.

$$M_{p,Rd} = N_{p,pl} \times \left(d_p - \frac{x_{pl}}{2} \right) + N_{s,pl} \times \left(d_s - \frac{x_{pl}}{2} \right) \quad (11)$$

The mechanical load is distributed over four lines of nodal loads (FY), with a spacing of 800 mm. This load represents the live load (used as parameter). The dead load is included by means of inertial effect (2800 N/m^2). The composite slab is considered to be simply supported (restraining the displacements in vertical and out-of-plane directions at the left support and restraining all displacements in the right support). The lines of nodal forces were applied in accordance to the experimental setup, see Figure 8.

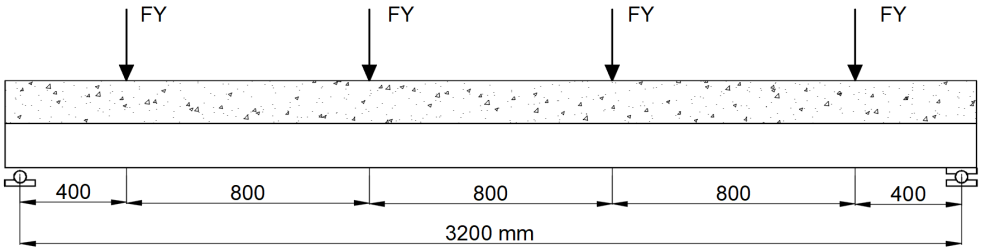

Figure 8. Representation of the mechanical model.

The dead load was calculated based on the volume and density of each material, using the inertial effect. The thermal load effect introduces the incremental time effect, using different files with the corresponding temperature field for each time step.

The finite element model uses a full three-dimensional finite element mesh, by switching the thermal SOLID70, SHELL131 and LINK33 finite element to the equivalent mechanical finite element SOLID185, SHELL181 and LINK180, see Figure 9.

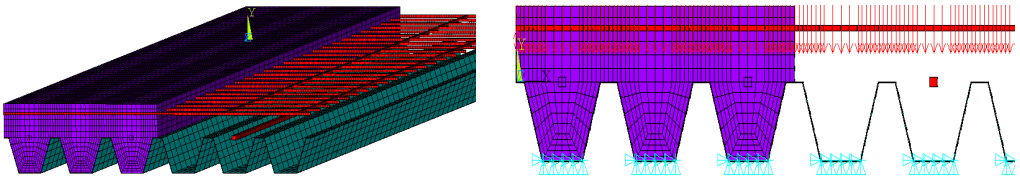

Figure 9. The finite element mechanical model.

SOLID185 is a three-dimensional finite element defined by eight nodes, having three degrees of freedom at each node (3 translations). This element uses linear interpolation functions and full

gauss integration. SHELL181 is a four-node element with six degrees of freedom at each node (3 translations and 3 rotations). This element also uses linear interpolating functions for in-plane with full integration scheme and linear interpolating functions in-thickness direction with 3 integration points. LINK180 is a unidirectional finite element with 2 nodes and 3 degrees of freedom at each node (translations). This element is superposed to the concrete nodes and uses 1 integration point.

The non-linear geometric analysis uses an incremental solution, based on Newton-Raphson method, with a convergence criterion defined by force and moment, with a tolerance value of 0.001 and a minimum reference value of 1. The elastic-plastic analysis was also used, considering the non-linear material behaviour. The concrete model is an adapted model form EN1992-1-2 [11]. The mechanical properties of the materials are temperature dependent and vary according to the standards used for composite slabs [6], steel structures [10] and concrete structures [11], see Figure 10.

The thermal expansion for each material was also considered in the model, due to the existence of a very high temperature gradient through thickness. This gradient is responsible for the existence of thermal bowing, increasing the rotation of the cross-section. The change of thermal expansion with temperature, denoted as the coefficient of thermal expansion, is not constant, especially for concrete. Due to shrinkage, the expansion of concrete stops at elevated temperatures (beyond 650 ºC). The expansion coefficient for steel has smaller variation with temperature. Changes in the microstructure explain the plateau between 750 and 800ºC.

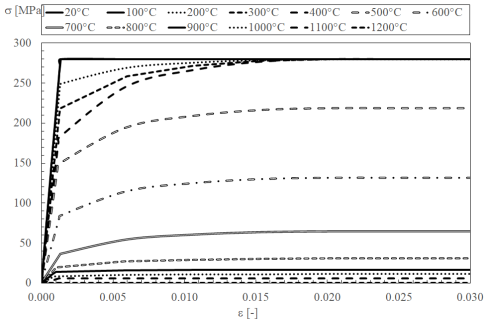

a) Mechanical properties of galvanized steel.

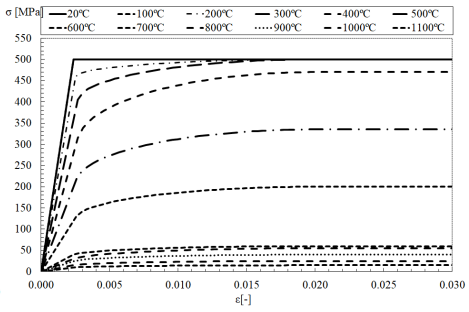

b) Mechanical properties of reinforcement.

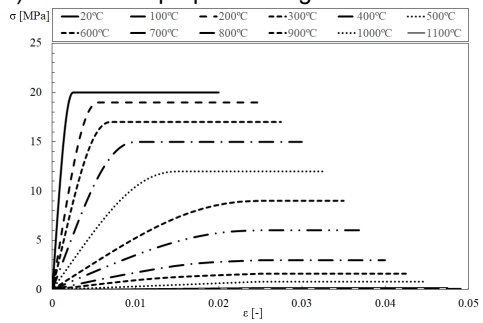

c) Mechanical properties of concrete.

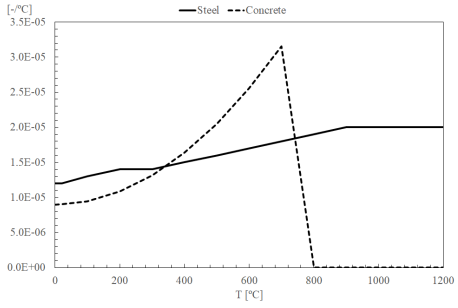

d) Coefficient for thermal expansion.

Figure 10: Mechanical properties for all materials.

4. RESULTS

The results of the three-dimensional numerical simulations are presented in this section, resulting from the application of the preceding models. The thermal analysis presents the results obtained with perfect contact (NUM 0) and with an air gap 1 mm thick between the steel deck and the concrete topping (NUM 1). These thermal results are compared with experimental results. A comparison of the fire resistance between the numerical, experimental and simple calculation method results is also presented. The thermo-mechanical numerical results are also compared with the experimental results. A parametric analysis was developed to determine the effect of the live load. A new proposal is presented for the fire resistance with respect to the load bearing criterion (R), and a comparison with the simple calculation method is also presented.

4.1 Experimental tests

An experimental test conducted by Hamerlinck [1] (test number 2) was selected to perform numerical simulations for both mechanical and thermal models. The slab was composed by the trapezoidal steel deck PRINS PSV 73 and a concrete topping with 70 mm thick using normal weight concrete. The simply supported slab was subjected to the ISO 834 standard fire. The profile of the composite slab is shown in Figure 2. The normal weight concrete was used for the composite slab and the measured moisture content of 3.5%.

4.2 Thermal simulation

Figure 11 illustrates the temperature development (numerical and experimental) at different points as well as the average and maximum temperatures at the unexposed side of the slab. Analysing the results, it can be observed that the temperature development on the selected points is quite similar between the experimental (EXPT) and the perfect contact model (NUM 0) at the first minutes of heating. Regarding the temperature development at point 2, the model with the air gap (NUM 1 – 1 mm) presents good approximation to the experimental results for temperatures over 100 °C. However, for the points 1 and 3, the perfect contact model presents better agreement with measured temperatures at the last minutes of heating. For the unexposed surface, the maximum and average temperature curves are very close for all the models. In this case, better agreement with the experimental results can be noticed using the model with the air gap.

It's important to list determining factors that have influence over the temperature of the composite slab during the initial stages of heating, for example, the existence of the moisture within the concrete that is partially solved by determining the variable specific heat of concrete in the ANSYS models, according to EN 1992-1-2 [11] (see figure 5), simulating the property value peak when temperature reaches 100°C but ignoring the influence of the evaporation of the water over the structure. Also, the existence of a zinc layer of the steel deck exposed face have influence over the beginning of the experimental tests that while the melting of the zinc occurs the reduction of heating increasing [13]. Solutions to this are proposed initially by Hamerlinck [1] and then adopted

by EN 1994-1-2 [6] determining a temperature variable emissivity (ε) to the steel deck directly exposed to fire that vary from 0,1 to 0,7 while the software ANSYS uses constant values to the element's emissivity. Thus this, initial delays on temperature increasing on steel deck are ignored on simulated models, but the results of simulations show that good convergence is guaranteed on later stages of tests on exposed face of the slab and during the hole simulation on the unexposed side.

Table 2 presents the results obtained for the fire resistance (criterion "I") of the slab with respect to the average temperature rise (t_{fi} Ave) and the maximum temperature rise (t_{fi} Max) at the unexposed surface. Obviously, for each model the lowest value between the two criteria governs the fire resistance.

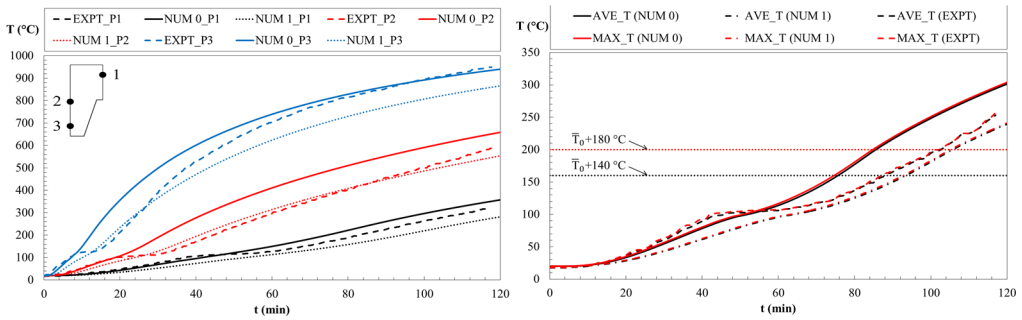

a) Selected points. b) Unexposed side.

Figure 11. Comparison between numerical and experimental results. Point 1, 2 and 3 at distance 20, 74 and 123 mm from the top.

Table 2: Fire resistance for insulation condition (I): experimental, numerical and analytical results.

	Model NUM 0	Model NUM 1	EXPT result	EN 1994-1-2 result
t_{fi} Ave (min)	75.6	93.5	88.2	106.5
t_{fi} Max (min)	84.8	105.1	102.1	

Assuming the experimental result as reference, it can be observed that the air gap model slightly overestimated the fire resistance, with a relative error of 6%. A bigger discrepancy is obtained using the perfect contact model, with a relative error of 14.3%. The EN 1994-1-2 provisions overestimated the fire resistance, providing an unsafe result with a relative error of 20.7%.

4.3 Mechanical simulation

In order to evaluate the fire resistance, the incremental and iterative solution is included. The maximum displacement and the rate of the maximum displacement should be analysed. Figure 12 represents the comparison between the experimental results and the numerical results. The critical time was determined by the first to achieve the limiting conditions presented in EN1363-1 [7].

The vertical displacement of the slab changes with time. The curvature of the slab starts increasing rapidly and deflections increase accordingly. In a second stage, the deflection rate decreases as thermal curvature increases less. Near the ultimate limit state, the deflection rate increases again due to the plastic material behaviour.

For the mechanical analyses, it should be highlighted that the thermal load was determined based on the perfect contact model between materials (NUM 0). That is, the effect of the air gap between the steel deck and concrete was not taken into consideration. This fact results in higher temperature values for the materials and explains the higher predicted values for the vertical displacement of the numerical results.

The normative simplified calculation, based on EN 1994-1-2 [6] results in overestimated resistance, given that, solving Eq. 5 to Hamerlinck laboured slab the load-bearing-criteria thermal resistance of R120 was determined. Experimental applied moment to the slab was 4640.06 N.m and the maximum sagging moment supported by it, according the normative, that was composed with normal weight concrete, to various resistance classes are shown in Table 3.

Table 3: Sagging moment capacity according fire resistance class to normal weight concrete (EN 1994-1-2 [6]).

Resistance Class (min)	Sagging Moment Capacity (N.m)
R60	11265
R90	8296
R120	5519

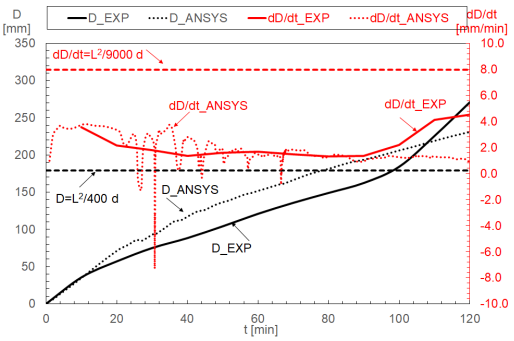

a) Time history for displacement and rate of displacement.

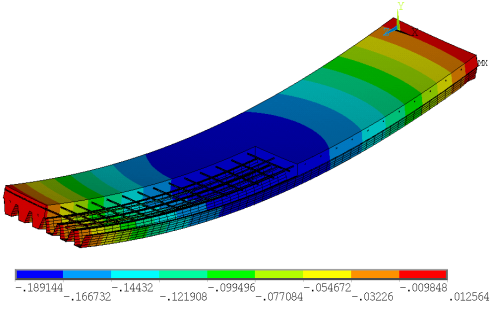

b) Deflection of the slab at the critical time.

Figure 12: Analysis of the composite slab with a live load of 2.7 kN/m².

Table 4 presents the comparison between the mechanical model with perfect contact and experimental results concerning the load bearing fire resistance.

Table 4: Fire resistance for load bearing condition (R): experimental, numerical and analytical results.

	Model NUM 0	**EXPT result**	**EN 1994-1-2 result**
t_{fi} D (min)	*78*	*97*	120
t_{fi} dD/dt (min)	Not achieved	Not achieved	

The difference between both results can be explained by several factors, mainly by the temperature field in each time step. Other parameters are also reported and are related with several phenomena during the test (variation of the view factors, creation of the air gap effect between the steel deck and concrete, restrain effect in the supports, direction of the applied load during the test, among others).

Results also show that the numerical model, compared to the EN 1994-1-2 exigencies [6] provide a conservative prevision of the slab mechanical behaviour under normal fire conditions. Yet, it is important to highlight the overestimated thermal resistance provided by the normative simplified calculation that could result in unsafe structures under fire conditions.

A parametric analysis was also developed, in order to verify the effect of the live load on the fire resistance. The load level, μ_0, was determined by the ratio of the total load (live and dead) by the plastic load at room temperature, proposed by the Eurocode 1994-1-1 [14]. The load varied from 1.0 kN/m^2 to 21.0 kN/m^2.

The fire resistance decreases with the load level, see Figure 13. The critical temperatures of the steel components were determined based on the fire resistance criteria. These values also decrease with the load level. The fire resistance for load bearing criterion was exclusively governed by the critical displacement value (D). The rate of displacement (dD/dt) did not reach the critical value for load level values below μ_0=43%. For higher load levels, the critical displacement rate becomes important, but never anticipates the time for the critical displacement. The thermal gradient can be easily determined for each load level, being approximately equal to 700 ºC/123 mm in the vertical direction. This value seems to be independent of the load level.

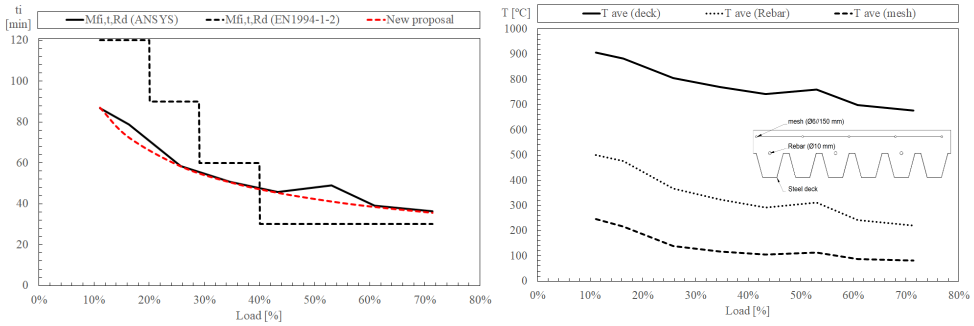

a) Fire resistance. b) Critical temperature.

Figure 13: Fire resistance of the composite slab and critical temperature for the steel components.

The fire resistance was approximated with the minimum safety level, considering the results of the new proposal bellow the line of the numerical results. The new formula is presented in Eq.11.

$$t_{fi} = 32.104\ \mu_0^{-0.464} - 2 \tag{11}$$

In practice, rebars should be applied to composite slabs with steel deck in cases when the required fire resistance time is higher than 30 minutes. When these elements are submitted to fire exposure, the contribution of the steel deck to the load bearing resistance decreases considerably, being part of this capacity transferred to the rebars.

5. CONCLUSIONS

This study presented the description of the thermal and mechanical three-dimensional finite element models as well as its validation against experimental data. The fire resistance according to the thermal insulation (I) and load bearing (R) criteria was determined and compared to experimental data as well as EN 1994-1-2 provisions. With the objective of simulating the effects of the debonding of the steel deck from concrete, an insulating layer (air gap) with a constant thickness of 1 mm was introduced between the concrete and steel deck.
Regarding the experimental results for the temperature development, a plateau at about 100 °C (due to moisture evaporation) should be highlighted, resulting in a decrease in the rate of temperature increase. The numerical results do not present this pronounced plateau possibly because localized moisture concentrations in the test may be higher than the uniform moisture content introduced in the model.

The fire resistance, with respect to the thermal insulation criterion, was governed by the average temperature rise criterion for both thermal models (NUM 0 and NUM 1) as well as for experimental results. The perfect contact model underestimates the fire resistance. In general, the results obtained with the air gap model presented better agreement with experimental results and satisfactorily simulated the debonding effect, reducing the temperature rise at the selected points and unexposed side as well. The EN 1994-1-2 provisions, for the fire resistance according to both thermal insulation criterion (I) and load-bearing criterion (R), were on the unsafe side, that is, the calculated fire resistance was greater than the measured one. Using the perfect contact model (NUM 0), the fire resistance with respect to the load bearing criterion was governed by the maximum displacement criterion. The numerical result underestimated the fire resistance due to the higher temperature field achieved with this model. The fire resistance decreases with the load level and a new proposal is presented. The proposed calculation model provides an optimization of these structures design when compared to the available standard EN 1994-1-2, suggesting safer components on buildings that requires lower load rates (μ_0), approximately 40% of capacity, and more economical solutions to structures which are usually solicited nearly it's maximum tolerance.

REFERENCES

[1] A. F. Hamerlinck, “The behaviour of fire-exposed composite steel/concrete slabs,” Eindhoven University of Technology, 1991.
[2] ISO, “Fire Resistance Test – Elements of Building Construction”, *International Standard ISO 834*, 1975.
[3] G. Thomson et al., “Indicative Fire Test on Composite Concrete/Steel Deck Floor System”, Steel Construction Institute, Rotherham, 1987.
[4] S. Guo & C. G. Bailey, “Experimental Behaviour of Composite Slabs During the Heating and Cooling Fire Stages”, *Engineering Structures*, Vol. 33, p. 563-571, 2011.
[5] CEN- European Committee for Standardization, *EN 13501-2: Fire classification of construction products and building elements – Part 2: Classification usig data from fire tests, excluding ventilation services*, CEN-Europ. Brussels, 2009.
[6] CEN- European Committee for Standardization, *EN 1994-1-2: Design of composite steel and concrete structures. Part 1-2: General rules - Structural fire design*. Brussels, 2005.
[7] CEN- European Committee for Standardization, *EN 1363-1: Fire resistance tests Part 1 : General Requirements*, CEN-Europ. Brussels, 2012.
[8] C. Both, “The fire resistance of composite steel-concrete slabs,” Technical University of Delft, 1998.
[9] J. Jiang, A. Pintar et al., “Improved calculation method for insulation-based fire resistance of composite slabs,” Fire Saf. J., vol. 105, pp. 144–153, Mar. 2019.
[10] CEN- European Committee for Standardization, *EN 1993-1-2: Design of steel structures - Part 1-2: General rules - Structural fire design Eurocode*. Brussels, 2005.
[11] CEN- European Committee for Standardization, *EN 1992-1-2: Design of concrete structures - Part 1-2: General rules - Structural fire design*, vol. EN 1992. Brussels, 2004.
[12] CEN- European Committee for Standardization, EN 1991-1-2, *Eurocode 1: Actions on structures – Part 1-2: General actions – Actions on structures exposed to fire*. Brussels, 2002.
[13] NIST, “Numerical Modeling and Analysis of Heat Transfer in Composite Slabs with Profiled Steel Decking”, *NIST Technical Note 1958*, National Institute of Standards and Technology, Gaithersburg, 2017.
[14] CEN- European Committee for Standardization, *EN 1994-1-1: Design of composite steel and concrete structures - Part 1-1: General rules and rules for buildings*. Brussels, 2004.
[15] G. M. E. Cooke et al., “Fire Resistance of Composite Deck Slabs”, *The Structural Engineer*, Vol. 66, 1988, p. 253-261.
[16] D. E. Wainman, “Summary of Data Obtained During Tests on Three Composite Metal Deck Shelf Angle Floor Beams”, *BS476 Fire Resistance Tests*, Part 21, Rotherham, 1996.
[17] CEN - European Committee for Standardization, *EN 1992-1-1: Design of concrete structures - Part 1-2: General rules and rules for buildings*, vol. EN 1992. Brussels, 2004.
[18] S. Guo, “Experimental and Numerical Study on Restrained Composite Slab During Heating and Cooling”, *Journal of Constructional Steel Research*, Vol. 69, p. 95-105, 2012.
[19] L. Lim et al., “Numerical Modelling of Two-Way Reinforced Concrete Slabs in Fire, *Engineering Structures*, Vol. 26, p. 1081-1091, 2004.
[20] L. C. S. Lim, “Membrane action in fire exposed concrete floor systems”, University of Canterbury, 2003.